Evidence from Amazonian forests is consistent with isohydric control of leaf water potential

ROSIE A. FISHER[1], MATHEW WILLIAMS[1], RAQUEL LOBO DO VALE[2], ANTONIO LOLA DA COSTA[3] & PATRICK MEIR[1]

[1]School of GeoScience, University of Edinburgh, Edinburgh, UK, [2]Instituto Superior de Agronomia, Tapada de Ajuda, Lisbon, Portugal and [3]Universidade Federal do Pará, Belém, Pará, Brazil

ABSTRACT

Climate modelling studies predict that the rain forests of the Eastern Amazon basin are likely to experience reductions in rainfall of up to 50% over the next 50–100 years. Efforts to predict the effects of changing climate, especially drought stress, on forest gas exchange are currently limited by uncertainty about the mechanism that controls stomatal closure in response to low soil moisture. At a through-fall exclusion experiment in Eastern Amazonia where water was experimentally excluded from the soil, we tested the hypothesis that plants are isohydric, that is, when water is scarce, the stomata act to prevent leaf water potential from dropping below a critical threshold level. We made diurnal measurements of leaf water potential (Ψ_l), stomatal conductance (g_s), sap flow and stem water potential (Ψ_{stem}) in the wet and dry seasons. We compared the data with the predictions of the soil–plant–atmosphere (SPA) model, which embeds the isohydric hypothesis within its stomatal conductance algorithm. The model inputs for meteorology, leaf area index (LAI), soil water potential and soil-to-leaf hydraulic resistance (R) were altered between seasons in accordance with measured values. No optimization parameters were used to adjust the model. This 'mechanistic' model of stomatal function was able to explain the individual tree-level seasonal changes in water relations ($r^2 = 0.85$, 0.90 and 0.58 for Ψ_l, sap flow and g_s, respectively). The model indicated that the measured increase in R was the dominant cause of restricted water use during the dry season, resulting in a modelled restriction of sap flow four times greater than that caused by reduced soil water potential. Higher resistance during the dry season resulted from an increase in below-ground resistance (including root and soil-to-root resistance) to water flow.

Key-words: drought; psychrometer; sap flow; SPA model; stem water potential; stomatal conductance.

INTRODUCTION

Over the next 50–100 years, most global climate models predict that increasingly El Niño-like climate conditions

Correspondence: Rosie A. Fisher. E-mail: rosie.fisher@ed.ac.uk

will cause reduced rainfall over Eastern Amazonia (Cox *et al.* 2000; Cubasch *et al* 2001; Cowling *et al.* 2004; Cramer *et al.* 2004). Cox *et al.* (2004) suggested that the reduction in rainfall over Amazonia may reach as high as 50% by 2100. Reductions in rain forest evapotranspiration during the dry season have been observed at Manaus, in relatively wet and humid Central Amazonia, by using the eddy covariance technique (Malhi *et al.* 1998, 2002). However, more recent eddy covariance studies in Eastern Amazonia have not shown any limitation in forest evaporation during the dry season, even though these forests experience more intense dry seasons than the Manaus forest (Carswell *et al.* 2002; Saleska *et al.* 2003; Goulden *et al.* 2004; da Rocha *et al.* 2004). The lack of a simple correlation between the limitation of forest evapotranspiration and the intensity of the dry season implies that we cannot simply extrapolate the results of a small number of experiments uniformly across the Amazon region. A more sophisticated understanding of the drought physiology of rain forest trees is necessary before we can predict the responses to the predicted drier conditions.

To investigate the mechanisms underlying the response of forest evapotranspiration to reduced rainfall, we conducted a manipulation study on a 1 ha parcel of land in Caxiuanã, Eastern Amazonia. Rain passing through the canopy (through-fall) was intercepted by a system of plastic panels and then drained away from the plot, thereby artificially reducing soil moisture. Within this through-fall exclusion (TFE) site and an adjacent control site, we collected diurnal cycles of leaf water potential (Ψ_l), stem water potential (Ψ_{stem}), stomatal conductance (g_s) and sap flow from a sample of trees during the wet and dry seasons. We used the tree physiology data to investigate three areas of uncertainty: (1) the mechanism by which the stomata sense and respond to soil water status; (2) whether leaf water supply is controlled by changes in soil water potential (Ψ_s) or in soil-to-leaf hydraulic resistance (R); (3) and whether major resistance to water uptake is located above or below ground.

The first part of our investigation involved testing the hypothesis that the stomata sense reduced soil moisture via 'hydraulic signalling' between soil water potential and leaf water potential (Jones 1998; Salleo *et al.* 2000; Chaves, Maroco & Pereira 2003). In this hypothesis, low soil mois-

ture affects stomatal conductance and gas exchange via its influence on leaf water potential. It has been repeatedly observed that some plants act to maintain leaf water potential above a critical minimum value, or 'isohydric' conditions, under hydraulically stressed circumstances (Field & Holbrook 1989; Tardieu 1993; Saliendra, Sperry & Comstock 1995; Cochard, Breda & Granier 1996; Comstock & Mencuccini 1998; Sperry *et al.* 1998, 2002; Oren *et al.* 1999; Bonal *et al.* 2000; Salleo *et al.* 2000; Hubbard *et al.* 2001). However, this does not mean that the water potential is constant at all times; rather, it suggests that because of stomatal closure, there exists a definite minimum value which the water potential does not exceed. The supposed primary role of this mechanism is the avoidance of low water potential, which leads to xylem cavitation (Jones & Sutherland 1991) and the possibility of runaway cavitation (Tyree & Sperry 1988). It has yet to be demonstrated that this isohydric behaviour is common in tropical forest trees, or that it can solely explain altered water use in whole trees between seasons.

As a complement to empirical testing, we used a modelling approach to investigate the ability of the isohydric hypothesis to explain the physiology of whole trees. In the field, stomatal conductance is high when both energy and water are abundant and stomata close due to either due to a lack of water, or due to a lack of energy (when the increase in photosynthesis to be gained by opening stomata is very small) (Farquhar *et al.* 1980)). Using a model allows us to dynamically link stomatal conductance, leaf water potential and energy availability to account for the multiple factors that determine stomatal conductance. The model we have used is the soil–plant–atmosphere (SPA) model (Williams *et al.* 1996). The SPA model is a multilayer soil–vegetation–atmosphere transfer (SVAT) model, the stomatal conductance algorithm of which is based on the isohydric hypothesis. We parameterized the SPA model, using measured estimates of hydraulic parameters, and compared the diurnal predictions of the model with the tree physiology data to test the isohydric hypothesis embedded in the model.

The second area of uncertainty investigated was whether soil water potential or soil-to-leaf hydraulic resistance was the factor that limits soil-to-leaf water supply under water-stressed conditions. Soil-to-leaf water transport, along with atmospheric demand, determines leaf water status, but it is not clear whether soil water potential or soil-to-leaf hydraulic resistance is the major factor that constrains water uptake during the dry season. Some previous modelling studies on tropical and seasonal temperate forests (Williams *et al.* 1996, 2001a) suggest that changes in ecosystem water use during the dry season could be explained only through changes in soil-to-leaf hydraulic resistance, as only small changes in soil water potential have been observed. However, other studies have found very large seasonal changes in soil water potential between seasons (Misson, Panek & Goldstein 2004). In this paper, we use measured estimates of soil water potential and soil-to-leaf hydraulic resistance, as well as the description of soil-leaf water trans-

port in the SPA model, to isolate the relative importance of both transport factors in constraining evapotranspiration during the dry season.

The third area of uncertainty investigated in this paper is the distribution of hydraulic resistance within the soil-to-leaf continuum. Soil-to-leaf hydraulic resistance consists of several hydraulic resistances in series in the leaves, branches, trunks, roots, root–soil interface and soil matrix. Much information exists describing the resistance of excised branch segments under different water potentials (Mencuccini 2002), but little information exists on the relative magnitudes of branch, trunk and below-ground resistance components (Sperry *et al.* 1998, 2002). It is impractical to obtain all information to model the dynamics of every resistance in the SPA continuum, it is more efficient to deduce the location of the major resistance to water transport. In this paper, we split the resistance of the soil-to-leaf pathway into above- and below-ground components using stem psychrometry measurements, and thus determine the location of the greatest resistance to water transport.

The following key questions are addressed in this paper:

1 Are the leaf water potential, sap flow and stomatal conductance data consistent with the hypothesis that stomata function to prevent leaf water potential declining below a minimum critical value under water stressed circumstances?
2 Are changes in soil-to-leaf water supply dominated by changes in soil water potential or by soil-to-leaf hydraulic resistance?
3 If there is a major change in soil-to-leaf hydraulic resistance between seasons, is the change in resistance located above or below ground?

We first address how the data alone may be used to answer these questions, then we investigate what additional conclusions we may draw, by comparing the data with the predictions of the SPA model.

METHODS

Site

The experimental site is located in the Caxiuanã National Forest, Pará, Brazil (1°43′3.5″S, 5°27′36″W). The forest is a lowland *terre firme* rain forest. The mean annual rainfall is 2272 mm (± 193 mm), but with a pronounced dry season between July and December, when on average only 555 mm (± 116 mm) of rainfall is recorded (data from 1999 to 2003). The soil is a yellow oxisol (Brazilian classification latosol), with a 0.3–0.4 m thick stony/laterite layer at 3–4 m depth. The soil texture (0.0–0.5 m) is 75–83% sand, 12–19% clay and 6–10% silt (Ruivo & Cunha 2003). The soil consists of mainly kaolin in the clay fraction and quartz in the sand fraction (Ruivo & Cunha 2003). The site elevation is 15 m above river level, and the water table has been observed at a depth of 10 m during the wet season.

TFE experiment

To investigate the limitation of soil water on forest gas exchange in drier conditions than those normally experienced, an artificial soil drought was created by using TFE. This work was carried out as part of the LBA (Large-Scale Biosphere Atmosphere Experiment in Amazonia) Ecology program (Avissar & Nobre 2002). Two 100×100 m plots, a control and a treatment TFE plot, were established, and the borders trenched to a depth of 1 m to reduce the lateral flow of water. In the TFE plot, a roof of transparent plastic sheeting and wooden guttering was installed at a height of approximately 2 m height in November 2001, to keep the soil free from rainfall.

A 30-m-tall canopy access tower was installed in each plot. Nine trees were accessible from each tower. Of these trees, five in the TFE plot and four in the control plot were equipped with sap flow monitors. The species, canopy heights and diameter at breast height (DBH) were recorded (Table 1). The sap-flow-equipped trees were the tallest trees accessible from the towers, and their leaves ranged from 11 to 28 m in height in the control plot and 16–28 m in the TFE plot. Trees were measured up to the top of the canopy. A meteorological station (Campbell Scientific, Loughborough, UK), installed on a 55-m-tall tower located 700 m from the experimental site, recorded climatic conditions [wet and dry bulb temperatures, rainfall, wind speed and direction, incoming and outgoing photosynthetically active radiation (PAR), short-wave and long-wave radiation] every 15 min.

Tree physiology measurements

Canopy leaf area index (LAI) was measured with an LAI-2000 Plant Canopy Analyser (Li-Cor, Inc., Lincoln, NE, USA) on a 10×10 m grid in both plots, in May 2003 and November 2003. The grid covered the full extent (100×100 m) of each plot. Diurnal courses of leaf water potential were monitored by using a digital pressure bomb (Skye Instruments, Llandrindnod Wells, UK) on 17 and 19 May 2003 (late wet season) and on 19 and 20 November 2003 (late dry season). On each of these days, four to five leaves were sampled from each of the intensively studied trees at 0600, 0900, 1100, 1300, 1500 and 1630 h, and leaf water potential was determined for each leaf by using the pressure bomb. Sap flow rates were measured for each of the intensively studied trees by using the trunk segment heat balance method (Environmental Measuring Systems, Brno, Czech Republic) (Cermak, Deml & Penka 1973; Cermak, Kucera & Nadezhdina 2004). The heat balance sensors measure sap flow over an entire sector of circumference, therefore they do not require calibration for xylem depth if the sensors (which are 30–50 mm long) penetrate through all of the active xylem tissue. Xylem depth was estimated in wood cores both visually and using dye previously injected below the point of measurement, to confirm that water was not transported beyond 30 mm depth. Xylem depth measurements of 47 trees, which ranged from 0.1 to 1.3 m in diameter, indicated that the xylem rarely extended beneath 20 mm depth, irrespective of tree size (data not shown); therefore, the 30-mm-long sap flow sensors cut through all of the conductive tissue. Water flux was logged every 15 min throughout each day.

The heat balance sap flow measurement method suffers from calibration errors around zero, such that when there is zero flow, a slight positive flow is recorded and a calibration is necessary. This is typically achieved by taking the minimum point over a period of several days and subtracting it from the raw data, so that the minimum becomes the zero point. This method is problematic if sap flow data are used to establish that the trees and soil have reached equilibrium, based on the achievement of zero sap flow during the night. However, if flow continues through the night as the leaves refill, then the flow will constantly decline as the soil–leaf water potential gradient becomes smaller. If flow were to stop altogether, then the apparent flow would be constant. For all of the trees studied the refilling period appeared to last only until between 2200 h and midnight. Thereafter, sap flow values remained constant to within 0.002 kg s^{-1} cm^{-1}. This constant value was used as the zero

Tree code	Species	DBH (m)	Ψ_{crit} MPa	Measurement height (m)	Canopy height (m)
C1	*Mezilaurus mahuba*	0.156	−1.9	11	6–21
C2	*Licania heteromorpha*	0.187	−0.9	19	18–26
C3	*Manilkara bidentata*	0.515	−4.3	28	21–30
C4	*Manilkara bidentata*	0.439	−2.7	27	23–31
T1	*Licaria ameniaca*	0.159	−2.2	16	10–22
T2	*Hirtela bicornis*	0.295	−2.1	20	15–30
T3	*Lecythis confertiflora*	0.366	−2.9	25	21–32
T4	*Swartzia racemosa*	0.485	−3.2	27	22–32

Table 1. Details of the intensively studied trees equipped with sap flow monitors and accessible from the canopy tower (C trees are the trees in the control plot, T trees are the ones in the TFE plot)

TFE, through-fall exclusion; DBH, diameter at breast height; $\Psi_{crit,}$ critical leaf water potential.

point in all cases, and the existence of unchanging sap flow for several hours was used as evidence of the existence of zero flow.

Stomatal conductance was measured using an LI-1600 leaf porometer (Li-Cor, Inc.). Diurnal measurements of the ambient transpiration rates, stomatal conductance and other associated meteorological variables (humidity, photon flux density, leaf and cuvette temperature) were made on the control plot on 27 May 2003 and on 31 October 2003, and in the TFE plot on 23 May 2003 and on 2 November 2003. (The May dates represent the late wet season while the October and November dates represent the late dry season.) Four to five leaves were sampled from each of the intensively studied trees. Measurement times were 0900, 1030, 1200, 1330, 1500 and 1630 h. Prior to 0900 h, very high (> 90%) humidity prevented accurate readings from being obtained from the porometer, because of low transpiration rates. Leaves were not divided into shade and sun leaves, because the sun/shade definition of a mid-canopy leaf changes very frequently as the position of the sun shifts throughout the day. It was assumed that at a given canopy level, all leaves experienced a similar proportion of sun and shade conditions.

Stem psychrometers (Plant Water Systems, Guelph, Ontario, Canada), in conjunction with a manual microvoltmeter (Wescor, Logan, UT, USA), were used to measure the water potential of the xylem at the base of each of the intensively studied trees. We collected these measurements at the same time as the leaf water potential measurements, in order to compare the water potentials of the leaves and stem. Prior to installation, the psychrometer sensors were calibrated against the pressure bomb measurements of leaf water potential. Nine leaves were collected from trees at different levels in the canopy at midday. From each leaf, a piece of the lamina was removed and measured with the psychrometers according to the Wescor protocol, while the water potential of the remaining leaf was measured by using the pressure bomb. After the calibration, we installed the sensors between the height of 0.2 and 0.3 m at the base of the intensively measured trees. The sensors were insulated with a foam with depth of 0.1 m and an aluminium foil radiation shield. This insulation was highly effective at removing temperature gradients between the two thermocouple junctions – the main source of error in psychrometer measurements – and the voltage gradient was never higher than 0.1 μV, which was within the range recommended by the manufacturers.

We measured the ambient hydraulic resistance of the excised segments of terminal branches during November 2002, May 2003 and November 2003 as another means of observing changes in above-ground hydraulic resistance. Four branches were collected from each intensively measured tree over several days. Branches were collected between 1400 and 1500 h to ensure that embolism risk was maximal. The leaves and petioles were removed immediately to prevent further water loss, and measurements were made within 3 h of collection to minimize the effects of cavitation recovery (Zwieniecki & Holbrook 2000). A low-pressure hydraulic resistance measurement system similar to that described by Sperry & Tyree (1988) was used to measure hydraulic resistance. Branch segments were between 0.09 and 0.15 m in length and 10–14 mm in diameter. Leaf area distal to each measured segment was found by measuring the area/mass ratio of a subset of leaves from each branch, using digital photography and Scion Image software (Scion Corporation, Frederick, MD, USA).

RESULTS

Meteorology

The average meteorology changed between the measured wet and dry season days (Fig. 1). The average air vapour pressure deficit (VPD) between saturation and the atmosphere over a 24 h period was higher in the dry season (0.5 kPa) than in the wet season (0.38 kPa). The average short-wave radiation increased from 183 W m^{-2} in the wet season to 216 W m^{-2} in the dry season. The average temperature was higher in the dry season (25.3 °C) than in the wet season (24.6 °C).

Sap flow

In the control plot, sap flow was 44% higher in the dry season than in the wet season. However, in the TFE plot, sap flow was 15% lower in the dry season than in the wet season (Fig. 2 and Table 2). The majority of the changes between seasons occurred in the upper canopy trees (C3, C4, T3 and T4). In particular, tree T3 showed a very large decline from 1134 to 16 kg d^{-1}. The sap flow data in Fig. 2 are normalized for tree leaf area (see modelling section), so differences between the trees are due to factors other than size.

Stomatal conductance

In control and TFE plots, the stomatal conductance of six out of the eight trees measured remained high (> 100 mmol m^{-2} s^{-1}) for the majority of the day during the

Table 2. Average daily sap flow value for the control plot (C) and TFE plot (T) trees during the wet and dry seasons

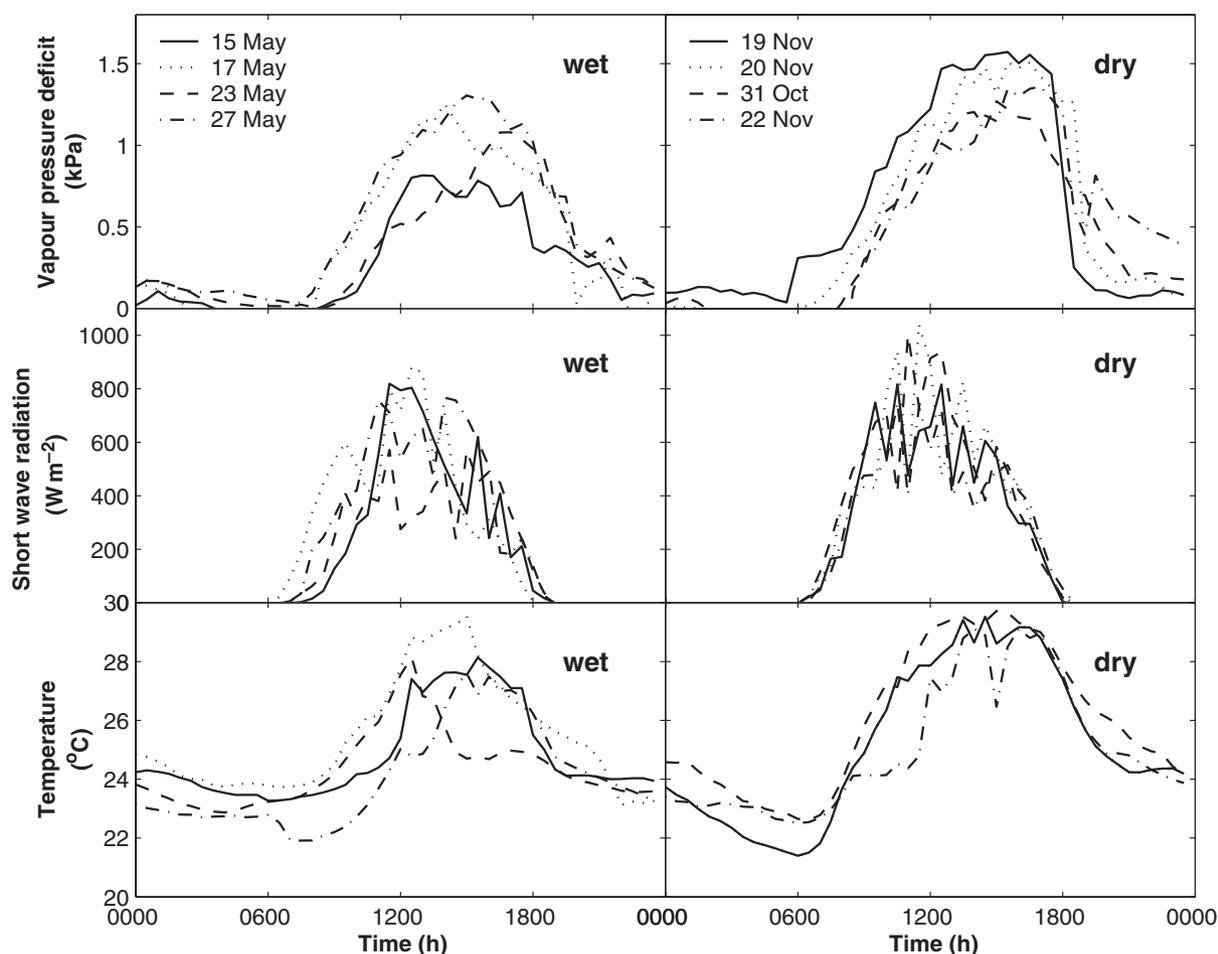| Plot	Tree code	Daily sap flow (kg d^{-1})	
		Wet season	Dry season
Control	C1	27	40
	C2	13	13
	C3	184	285
	C4	438	777
TFE	T1	40	45
	T2	34	45
	T3	134	16
	T4	157	134

TFE, through-fall exclusion.

Figure 1. Diurnal courses of vapour pressure deficit, short wave radiation and air temperature at 30 m height on wet season days (15, 17, 23 and 27 May 2003) (left-hand panels) and dry season days (19 November, 20 November, 31 October, 2 November 2003) (right-hand panels).

wet season (Fig. 3). Average maximum stomatal conductance was 184 mmol m^{-2} s^{-1} and the only period with low (< 100 mmol m^{-2} s^{-1}) stomatal conductance occurred at 1630 h in the TFE plot, which corresponds to a period of low radiation and temperature (Fig. 1). In the dry season, g_s was 35 and 39% lower than in the wet season in the control and TFE plots, respectively. In the dry season, g_s declined gradually between 0900 and 1530 h in the control plot, but no diurnal pattern was observed in the TFE plot, and g_s remained between 45 and 85 mmol m^{-2} s^{-1} for the whole day.

Leaf water potential

We found that the daytime leaf water potentials were lower in the dry season than in the wet season for both plots (Fig. 4). The average minimum leaf water potential reached was −1.71 MPa in the wet season, and −2.47 MPa in the dry season. For each measurement period, there was no significant difference in daytime leaf water potential values between plots ($P > 0.05$). During the dry season, leaf water potential declined quickly each morning in all trees, reach-

ing a plateau around a minimum value by 0900 or 1100 h and remaining within 0.5 MPa of the minimum value for the majority of the day (from 0900 or 1100 h until at least 1500 h). The exception to this was tree C1, which showed gradual recovery in leaf water potential throughout the afternoon of 20 November. However, this tree did display a minimum plateau around −1.7 MPa on the 19th November, below which it did not decline at any other time. Between 1500 and 1630 h, leaf water potential recovered slightly in six out of the eight trees studied. We found large differences in the minimum leaf water potential values reached by the different trees (Table 1). The minimum leaf water potential reached was negatively correlated with height ($r^2 = 0.74$). In the wet season, none of the trees reached the same minimum level observed in the dry season (with the exception of tree T2).

Stem water potential

The calibration procedure showed that the psychrometers provided an unbiased estimate of stem water potential. Regression analysis of the data indicated that very little
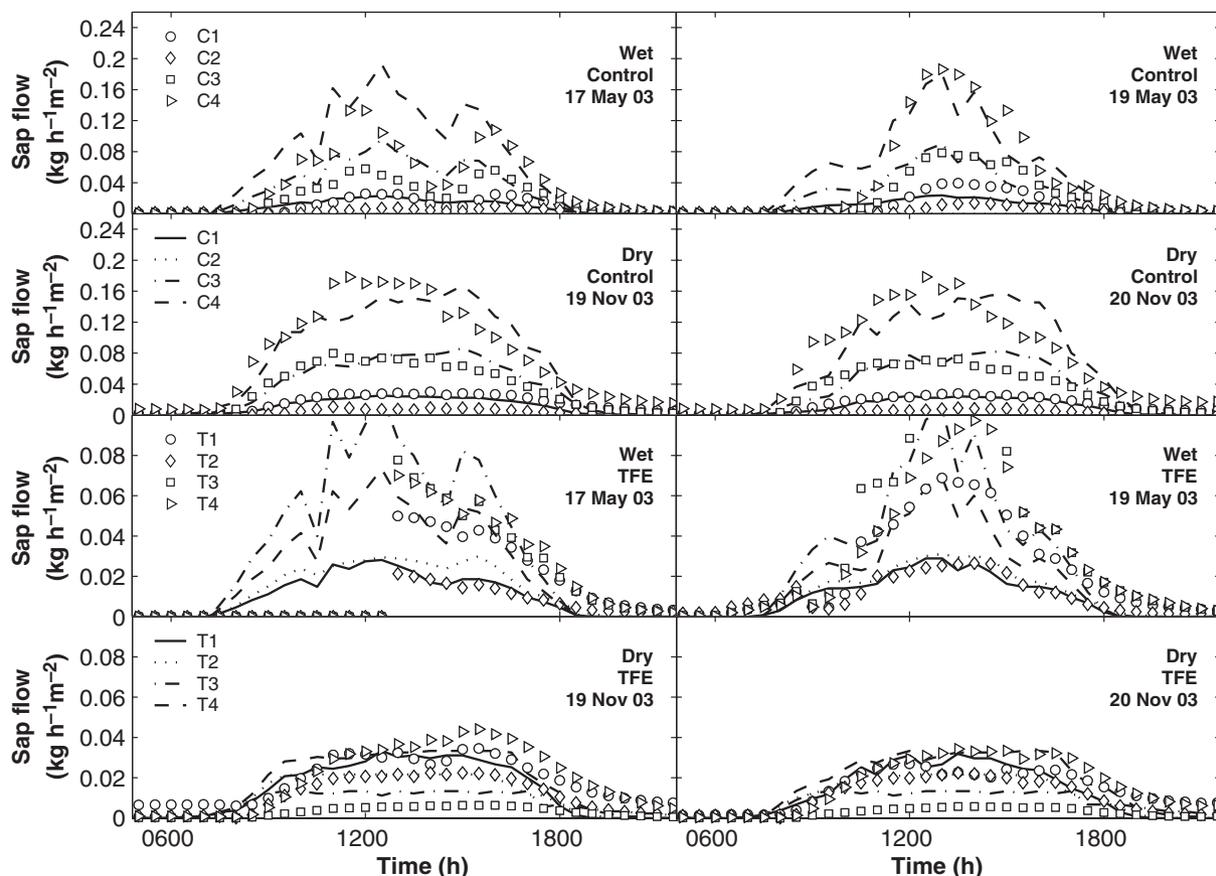
Figure 2. Measured (symbols) and modelled (lines) sap flow per m^2 leaf area for individual trees in the control (top four panels) and through-fall exclusion (TFE) (bottom four panels) plots for wet and dry seasons. C1–C4 are trees in the control plot and T1–T4 are trees in the TFE plot. Note the change in scale between control and TFE plot figures.

calibration was necessary, as the slope of the psychrometer/pressure bomb relationship was 1.03 and the intercept was 0.092 MPa with an r^2 value of 0.94, thus indicating that the psychrometers provided a reliable estimate of leaf water potential compared with that of the pressure bomb. In other investigations, stem psychrometers have been calibrated against sections of wood that are subject to drying (Irvine & Grace 1997). In this instance, the variability of tree species and the logistics of felling large rain forest trees meant that this approach was not possible. We were therefore limited to calibration against leaf laminar measurements. In this case, however, virtually no correction was made to the psychrometer outputs following calibration. It is feasible that an error in the psychrometer measurements could have been introduced as a result of measurements being made on woody stems instead of leaf laminae. In the wet season, the values of stem water potential were consistently higher than −0.5 MPa, close to the values of soil water potential estimated from pre-dawn leaf water potential (−0.08 to −0.09 MPa). In the dry season, the data on stem water potential show similar plateaux to the leaf water potential measurements (Fig. 5), with the levels of the plateaux being slightly (0.7 MPa average difference) wetter

than the values of leaf water potential. The average dry season stem water potential was −1.69 MPa in the control and −1.53 MPa in the TFE plot.

Branch resistivity

We found no difference in the ambient resistivity of the excised terminal branch segments between seasons (Fig. 6), but there were large differences between the resistivity values for the different trees. The highest resistivity (0.37 m^{-2} s MPa mmol^{-1}), which was recorded for tree C1, was 9.4 times higher than the least resistivity (0.04 m^{-2} s MPa mmol^{-1}), which was recorded for tree C3.

Modelling

Justification of modelling exercise

The data presented here indicate, from an initial analysis, that they are broadly consistent with the isohydric hypothesis that the stomata respond to leaf water potential in order to prevent leaf water potential from decreasing to a
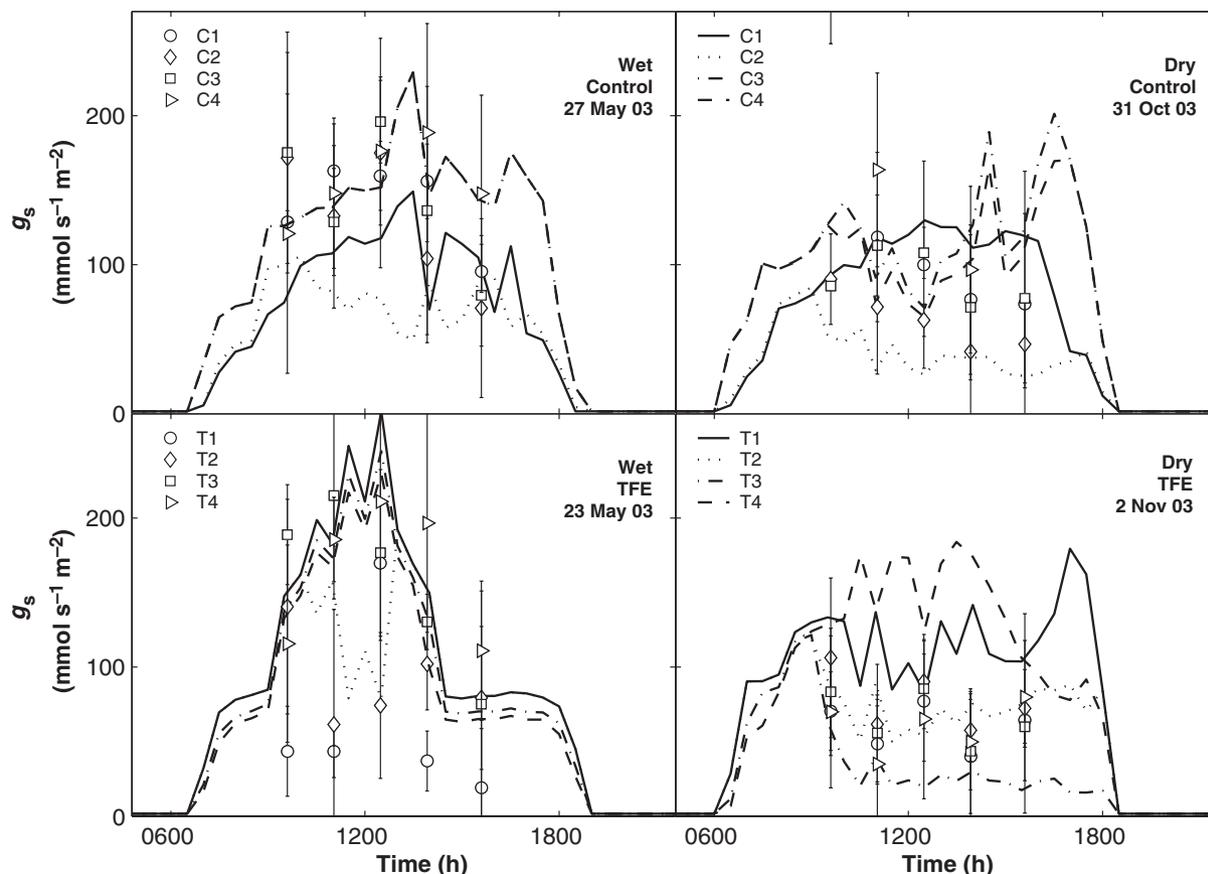
Figure 3. Measured (symbols) and modelled (lines) stomatal conductance for individual trees in the control (top two panels) and throughfall exclusion (TFE) (bottom two panels) plots for wet and dry seasons. C1–C4 are trees in the control plot and T1–T4 are trees in the TFE plot.

level below a critical threshold value under water-limited conditions. A persistent minimum leaf water potential plateau was observed during the dry season in all trees. When the leaves were at their minimum leaf water potential during the dry season, the stomatal conductance was consistently low. During the wet season, high stomatal conductances were observed and the leaf water potential was not near the minimum value.

However, the leaf water potential data alone do not actually confirm the existence of an isohydric mechanism. The plateaux in leaf water potential could possibly have been due to the meteorological conditions, for example, low atmospheric demand for moisture may have caused the fortuitous maintenance of stable leaf water potentials. To exclude this possibility, we must establish that the atmospheric demand at all the different canopy levels was high enough to reduce leaf water potentials to a level below the measured values, in the absence of stomatal control. Therefore, construction of the predictions of the isohydric model necessitated the use of a dynamic simulation model. We chose to use the SPA model (Williams *et al*. 1996) to simulate the predictions of the isohydric hypothesis for each data set for the following reasons:

1 The isohydric hypothesis proposes that leaf water potential is the dominant control over stomatal conductance and water use in water-limited conditions. Leaf water potential is the balance of soil-to-leaf water supply and atmospheric loss. To generate 'expected' leaf water potential values, we must simultaneously model both atmospheric demand and soil-to-leaf water supply. Both these processes are explicitly simulated by the SPA model.

2 Stomatal conductance may be limited either by hydraulic stress or by low light energy levels. Therefore, to predict the model expectations of stomatal conductance, we need simulations of both the leaf water potential and the availability of light energy to the leaves. The SPA model includes a radiative transfer scheme and a model of leaf water potential to allow both the factors that determine stomatal conductance to be simulated.

3 Tree-level predictions of sap flow must be constructed from leaf level estimates of evapotranspiration. Leaves at different heights in the canopy of a single tree have different rates of sap flow depending on their respective energy supply and hydraulic limitation. The SPA model includes a multilayer model of the forest canopy and a radiative transfer model, so it is possible to scale from leaf-level evapotranspiration predictions to tree-scale
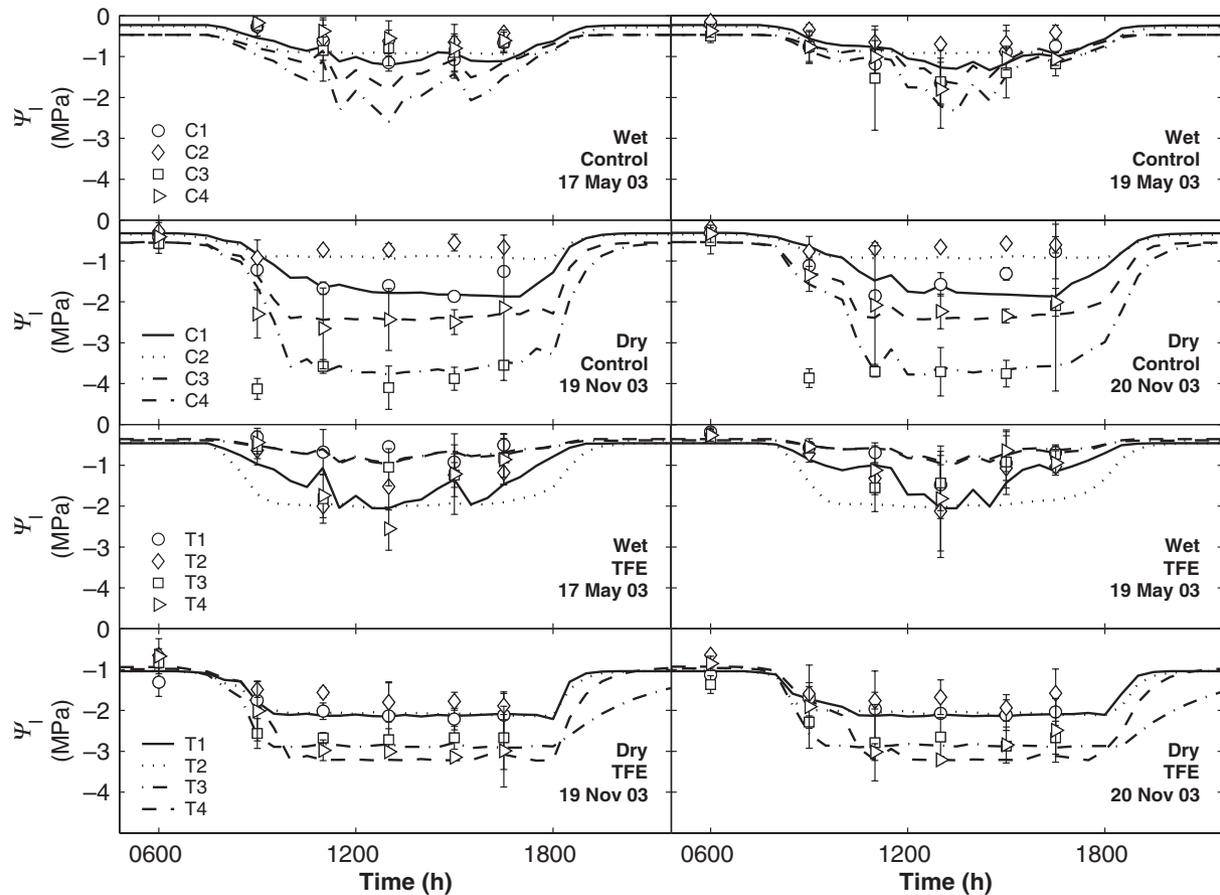
Figure 4. Measured (symbols) and modelled (lines) leaf water potential for individual trees in the control (top four panels) and through-fall exclusion (TFE) (bottom four panels) plots for wet and dry seasons. C1–C4 are trees in the control plot and T1–T4 are trees in the TFE plot.

sap flow predictions, therefore producing patterns of sap flow that are consistent with the isohydric hypothesis.

4 Prediction of stem water potential from leaf water potential is difficult, because water storage, or capacitance, in the tree leads to a lag between the leaf water potential and the stem water potential measured at the base of the tree in the morning, as water is supplied from above the ground and not drawn from the soil. Estimates of stem water potential dynamics consistent with the hypothesis can be made by using a dynamic model of the interaction between capacitance and resistance that has been incorporated into the SPA model.

The SPA model

The SPA model is a multilayered SVAT model that is designed to represent processes that are common to vascular plants, so that ecosystem–atmosphere exchange may be understood in terms of similar processes in different locations. The model has previously been tested in temperate deciduous and evergreen forests, arctic tundra and tropical rain forest ecosystems (Williams *et al*. 1996, 1998, 2000, 2001a; Williams, Bond & Ryan 2001b).

SPA is ideally suited to investigating the impact of drought on forest ecosystems because of its explicit modelling of water transport to leaves. In the model, stomatal conductance is controlled such that photosynthesis is maximized while not allowing leaf water potential to drop below a critical minimum value. If leaf water potential (Ψ_l) reaches the critical minimum leaf water potential (Ψ_{crit}), stomatal conductance (g_s) decreases and further water loss is prevented, therefore causing isohydric model behaviour under water-stressed conditions. Leaf water potential is determined from the balance of atmospheric demand, simulated by using the Penman–Monteith equation (Jones 1992), and leaf water supply, as shown in Eqn 1.

$$\frac{\delta \Psi_l}{\delta t} = \frac{\Psi_s - \rho g h - ER - \Psi_l}{CR}, \tag{1}$$

where Ψ_s is the soil water potential, ρ is the density of liquid water (kg m^3), g is gravitational acceleration (9.8 m s^{-2}) and h is the height (m) of the canopy layer. Strictly, this should be the vertical distance between the point of water uptake and the leaves. However, we are, at this stage, unsure of the height of the water uptake and therefore are not able to correct for these changes. However, a 10 m difference in
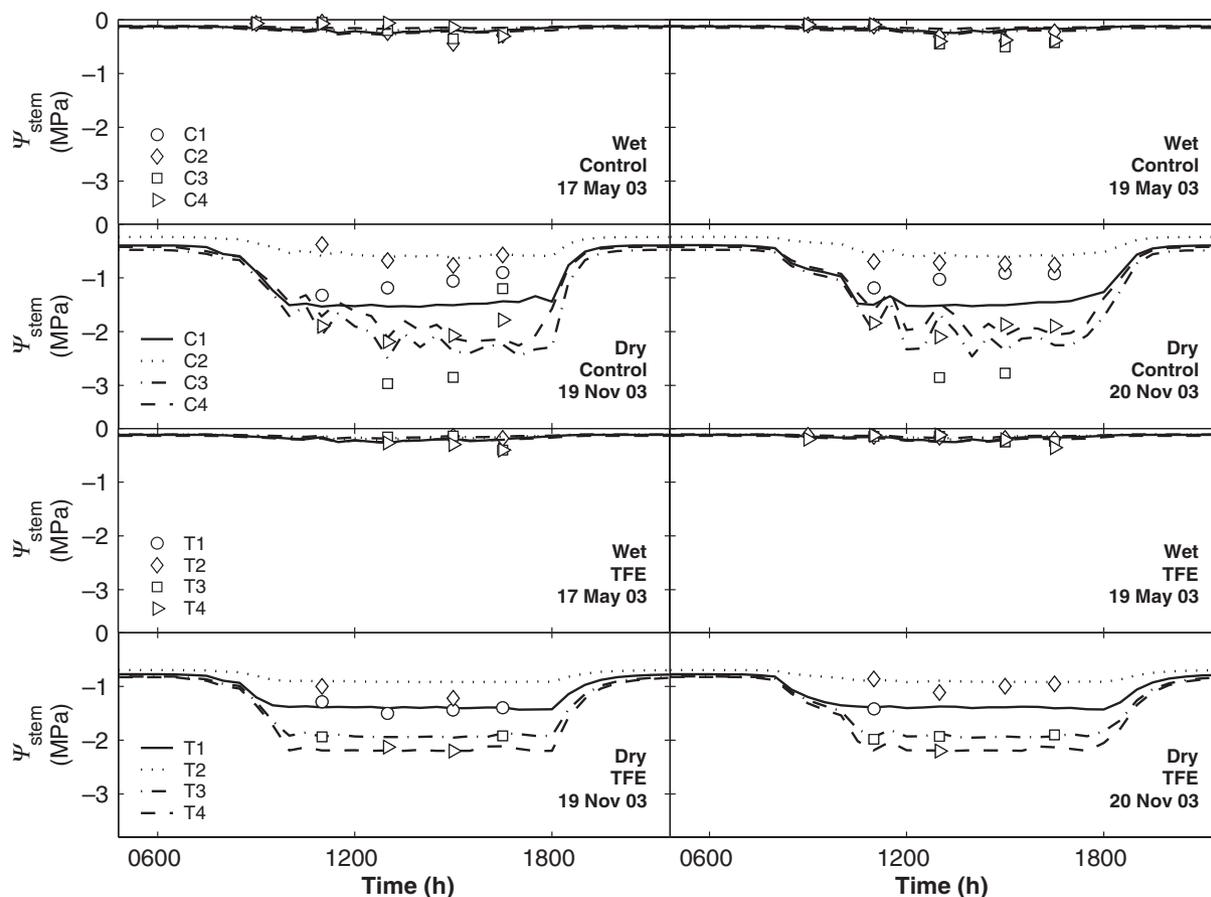
Figure 5. Measured (symbols) and modelled (lines) stem water potential for individual trees in the control (top four panels) and through-fall exclusion (TFE) (bottom four panels) plots for wet and dry seasons. C1–C4 are trees in the control plot and T1–T4 are trees in the TFE plot.

height causes only a 0.1 MPa difference in gravitational leaf water potential, so this is thought to be of little consequence in relation to the observed changes in leaf water water potential in all trees. *E* is the rate of evapotranspiration (mmol m^{-2} s^{-1}), *C* is the capacitance (mmol m^{-2} MPa^{-1}) and *R* is the soil–leaf hydraulic resistance (m^{-2} s MPa mmol^{-1}). To solve this equation, we must first define the hydraulic properties that determine water supply to the leaves, *R*, *C* and Ψ_s. All these parameters are physical properties of trees or ecosystems and can be estimated either independently or, in the case of *R*, from a subset of the data. The hypothesis underlying the SPA stomatal conductance algorithm has not been previously tested against high-resolution diurnal time series tree physiology data as presented here.

Models inputs

We ran the SPA model for each tree for each of the intensively measured days. All parameters in SPA remain as given by Williams *et al*. (1996) unless stated otherwise. Of those inputs that were changed to reflect local observations, some were common to all trees, plots and seasons, and others were varied according to available data (Table 3).

C was estimated as 2300 mmol MPa^{-1} m^{-2} from measurements made by Goldstein *et al*. (1998) for a seasonal tropical forest in Panama, the only published estimate of *C* for tropical forest trees (see Appendix) and was assumed to be constant between seasons. Ψ_s was determined from the averaged pre-dawn Ψ_l measurements (Fig. 4), for each plot and season. Sap flow decreased to zero during the night (Fig. 2), indicating that equilibrium between the soil and tree had been reached, so pre-dawn Ψ_l should be a reasonable estimate of Ψ_s (Donovan, Linton & Richards 2001). LAI was determined from the LAI-2000 measurements (Table 3). Ψ_{crit} was determined for each tree from the minimum observed leaf water potential (Table 1) and was kept the same between seasons.

Soil-to-leaf hydraulic resistance (m^2 s MPa mmol^{-1}) varies between trees and seasons, and was calculated as shown in Eqn 2.
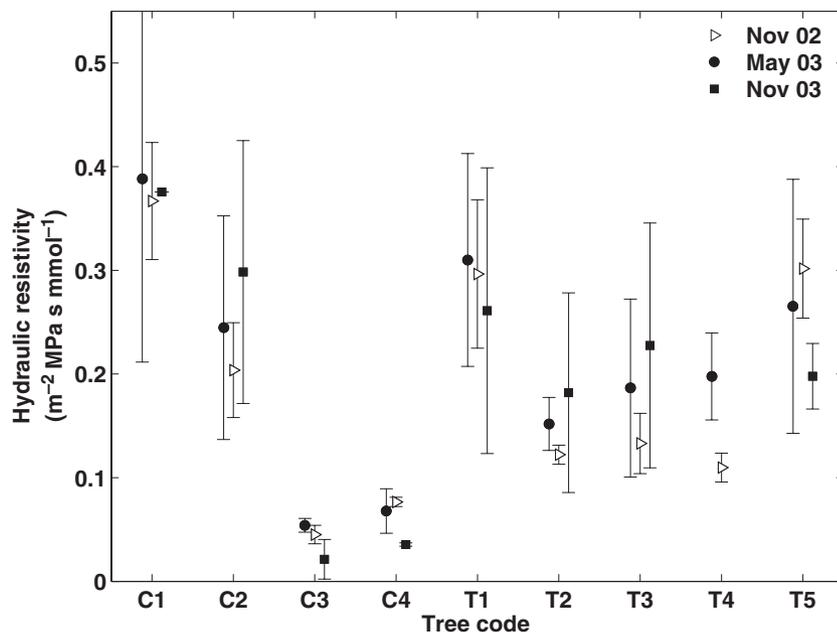
Figure 6. Resistivity of excised branch segments in the November (dry season) of 2002 and 2003 and May (wet season) of 2003. Measured using the method of Sperry (1988) for branch segments 0.09–0.15 m long and 10–14 mm in diameter. Error bars are standard deviation of four measurements.

$$R = \frac{A(\Psi_l - \Psi_s)}{S} \tag{2}$$

where S is the tree-level sap flow (mmol s^{-1}) and A is the tree leaf area (m^2) calculated from the tree diameter. The diameter was assumed to be proportional to leaf area since we found no relationship between xylem depth and tree diameter. The ratio between diameter and leaf area was derived from the tree survey diameter data and canopy LAI. We estimated R from each measurement of Ψ_l. The estimates of R at 0900 h were very high, since the release of stored water from plant tissues above the sap flow sensor allowed Ψ_l to drop without causing a corresponding increase in sap flow rate and thus creating a high apparent resistance. Thereafter, R reached a plateau that is stable to within 1 m^2 s MPa mmol^{-1}. We took the average value of this post-0900 h plateau and used it as the R parameter in the model (Table 4).

The SPA model inputs were independent of the verification data, with the exception of three parameters, Ψ_{crit}, Ψ_s and R. However, all three of these parameters were found

deterministically, by using the methods previously described. Critically, these parameters were determined without reference to the fit between the model and the data; therefore, they are not 'fitted' or 'optimized' parameters but representations of real physical or biological properties.

Processing of model output for comparison with data

The SPA model provided predictions of gas exchange and physiology for layers of leaves at different heights in the canopy. Leaf water potential and stomatal conductance data were compared directly with the model output at the height at which they were measured. To allow comparison of the tree-level sap flow data with the model output, the leaf-level model predictions were scaled to the tree level. We again allocated a total leaf area to each tree (A) and distributed it evenly between the lowest and highest canopy layers occupied by each tree (Table 1). Sap flow was estimated for each layer from the SPA model predictions, and

Table 3. Characteristics of the control and TFE plot used as input to the SPA model.

Parameter	Units	Control		TFE		Source
		Wet	Dry	Wet	Dry	
Canopy height	m			30		Measurement from tower
Capacitance	mmol m^{-2} MPa^{-1}			2300		Goldstein *et al.* (1998)
Soil water potential	MPa	−0.09	−0.17	−0.08	−0.66	Pre-dawn Ψ_l
LAI	m^3 m^{-3}	5.0	5.8	4.3	4.6	LAI 2000

Some parameters were constant between seasons (canopy height and capacitance) and some were varied between seasons according to measured values (LAI, soil water potential).

TFE, through-fall execution; SPA, soil–plant–atmosphere; Ψ_l, leaf water potential; LAI, leaf area index.

Parameter	Units	Season	Control plot				TFE plot			
			C1	C2	C3	C4	T1	T2	T3	T4
R	m^{-2} s MPa mmol^{-1}	Wet	2.0	3.0	1.1	0.6	1.1	3.7	0.5	0.8
		Dry	2.8	3.0	4.1	2.5	2.1	3.5	19.7	6.1
b	–	Wet	0.1	0.1	0.2	0.1	0.1	0.1	0.1	0.2
		Dry	0.6	0.2	0.9	0.8	0.3	0.1	0.7	0.6
R_{ag}	m^{-2} s MPa mmol^{-1}	Wet	1.8	2.7	0.9	0.5	1.0	3.3	0.5	0.6
		Dry	1.1	2.4	0.4	0.5	1.5	3.1	5.9	2.4
R_{bg}	m^{-2} s MPa mmol^{-1}	Wet	0.2	0.3	0.2	0.06	0.1	0.4	0.05	0.2
		Dry	1.7	0.6	3.7	2.0	0.6	0.3	13.8	3.7

Table 4. Values of R (soil-leaf hydraulic resistance) calculated using Eqn 2, b (the proportion of resistance located below ground) fitted to the Ψ_{stem} data, and the R_{ag} and R_{bg} (above- and below-ground resistance, respectively) calculated from the values of R and b

TFE, through-fall exclusion.

the tree-level sap flow was the sum of all the sap flow from the individual layers (see Appendix for full details of the scaling approach).

To compare the predictions of the isohydric hypothesis, as embedded in the SPA model, with the data on stem water potential, we used the SPA model output of Ψ_l to create estimates of modelled stem water potential for each tree. However, stem water potential depends not only on Ψ_l and Ψ_s but also on the distribution of hydraulic resistance above and below ground, b, which can be obtained through Eqn 3.

$$b = \frac{R_{bg}}{R} \qquad (3)$$

where R_{bg} is the leaf-specific hydraulic resistance located below ground, in the roots and soil, and R is the total soil-to-leaf hydraulic resistance (both m^2 s MPa mmol^{-1}). To find the value of b, which best explained the stem water potential data, we created several different scenarios of the modelled stem water potential, with values of b ranging from 0 and 1, in increments of 0.1. We calculated the modelled stem water potential, as shown in Eqn 4.

$$\Psi_{stem} = [b(\Psi_l - \Psi_s)] + \Psi_s \qquad (4)$$

where Ψ_l and Ψ_{stem} are the modelled leaf and stem water potential, respectively, and Ψ_s is the soil water potential estimated from pre-dawn leaf water potential. We then determined which value of b gave rise to the smallest root mean square error (RMSE) between the modelled and measured Ψ_{stem} values. The value of b, fitted in this manner, is therefore an estimate of the proportion of the soil-to-leaf resistance which was located below ground in each season. We then estimated the absolute values of the above- and below-ground resistance (R_{ag} and R_{bg}, respectively) by multiplying the total soil–leaf resistance (R) by the proportion located below ground (b) or above ground ($1 - b$).

Model sensitivity to wet–dry season input changes

Water supply to leaves, at a given leaf water potential, depends on soil-to-leaf hydraulic resistance and soil water

potential. It is unclear which of these two factors change the most between seasons and which has the greatest impact on water supply within the range experienced. In addition, sap flow rates are influenced by meteorology and LAI changes. We used the SPA model to investigate which of these factors was the dominant cause of altered sap flow between seasons, by generating SPA output for each plot six times. For the 'baseline' run, we used wet season input values of LAI, Ψ_s, R and meteorology data (Table 4). For the second run, we altered the meteorology data to its dry season value to test the impact of increasing temperature, VPD and solar radiation. The remaining four model runs tested the impact of altering the LAI, Ψ_s and R to their dry season values (Table 5, column 1). In each instance, we estimated the canopy sap flow, averaged for the two modelled days in each season and for the four tree-specific parameterizations. This allowed us to create a stepwise estimate of the effect of the different variables on the total sap flow.

Model verification

The isohydric hypothesis, as incorporated into the SPA model, showed good agreement with the data in the

Table 5. Modelled average daily sap flow in mm d^{-1}

Variables included	Control plot	TFE plot
Baseline	3.4	3.7
Met	4.2	4.6
Met + LAI	4.3	4.7
Met + LAI + Ψ_s	4.2	4.4
Met + LAI + R	4.0	3.6
Met + LAI + Ψ_s + R	3.9	3.1

Baseline refers to the predictions made using wet season meteorology data and parameters. The model inputs were then sequentially changed to their dry season values to identify which factor was the main cause of interseason variation in water use. Differences between plots in the baseline values are due to differences in wet season LAI.
TFE, through-fall exclusion; Met, meteorology data; LAI, leaf area index; Ψ_s, soil water potential; R, soil-leaf hydraulic resistance.

majority of cases. The model accounted for an average of 85% of the variation of Ψ_l, 83% of the variation of sap flow, 57% of the variation in g_s and 98% of the variation in Ψ_{stem} (Table 6). In the wet season, stomata were fully open, leaf water potential did not drop down to the minimum value and sap flow values were high (Fig. 4). In the dry season, as a result of changes in model inputs (R, Ψ_s and LAI) and meteorological drivers, the SPA model captured the reduction in leaf water potential to the minimum value in all trees (Fig. 4), and the resulting reduction in stomatal conductance (Fig. 3). The reduction in g_s in the TFE plot was strong enough to cause a large reduction in the sap flow of the TFE plot trees, in agreement with the data (Fig. 2). In the control plot, the stomatal closure necessary to maintain the minimum leaf water potential was not sufficient to cause a major decline in sap flow rates, and in fact, the rising VPD meant that sap flow increased in the control plot in the dry season, again in agreement with the data. Other features of the data that were well described by the model include the reduction in the rate of sap flow during the evening (this is codependent on the resistance and capacitance values) and the difference in leaf-area-specific sap flow between trees, which occurs as a result of their different illuminations at different heights in the canopy. Predictions of the magnitude of reduction in leaf water potential in the wet season, when no hydraulic limitation is present, agrees with the data.

One inconsistency between the model hypothesis and the data is that a modelled increase in stomatal conductance was found on several of the trees at 1630 h during the dry season (Fig. 3), when no increase in stomatal conductance

Table 6. r^2 and slope values of the relationship between data and the SPA model predictions of leaf water potential, sap flow, stomatal conductance and stem water potential for individual trees Data for different seasons are combined

Parameter	Tree	Ψ_l	Sap flow	g_s	Ψ_{stem}
r^2	C1	0.78	0.90	0.39	0.98
	C2	0.83	0.90	0.74	0.92
	C3	0.80	0.92	0.29	0.93
	C4	0.89	0.90	0.90	0.97
	T1	0.85	0.72	0.70	0.99
	T2	0.87	0.81	0.38	0.99
	T3	0.94	0.72	0.87	0.99
	T4	0.91	0.75	0.30	0.99
Slope	C1	0.73	1.06	1.34	0.71
	C2	0.73	0.91	1.24	1.11
	C3	0.92	0.79	0.49	1.11
	C4	0.99	0.85	1.05	0.98
	T1	1.00	1.02	0.53	1.01
	T2	0.89	0.63	0.26	1.12
	T3	0.81	0.71	0.71	1.00
	T4	0.81	0.88	0.42	0.99

Data for different seasons are combined.
SPA, soil–plant–atmosphere; ψ_l, leaf water potential; g_s, stomatal conductance; ψ_{stem}, stem water potential.

has been observed in the data. This coincides with a recovery in leaf water potential in both the model and the data (Fig. 4). This indicates that in the model the energy available was sufficient to justify some stomatal opening in the late afternoon. However, the data show that the trees did not respond to the removal of hydraulic limitation in the same manner. The data therefore indicate that some further stomatal closure mechanism may be necessary to explain the observed stomatal behaviour.

DISCUSSION

Are the leaf water potential, sap flow and stomatal conductance data consistent with the hypothesis that the stomata function to maintain isohydric conditions within the plant under water-stressed circumstances?

The isohydric hypothesis, as embedded in the SPA model, produced results that were broadly consistent with the data. Importantly, the SPA model contains no 'optimized parameters', or parameters whose value is adjusted to minimize the model-data error. A minimum plateau of leaf water potential was observed during the dry season in the majority of cases, at the same time as reduced stomatal conductance was observed. The SPA model analysis indicates that these patterns are consistent with a hypothesis of hydraulic limitation and not of reduced atmospheric demand or light availability. Because the model is based on underlying physical factors, we have been able to use it to test the physiological hypothesis underlying stomatal function, with encouraging results.

The main consistent exception to the isohydric hypothesis was the afternoon stomatal opening which the SPA model predicted for some trees in the dry season but was not observed in the data. There are at least two possible explanations for the observed lack of afternoon stomatal reopening in the absence of hydraulic stress. Firstly, there is a direct response of stomata to VPD, such that the VPD observed at 1600 h during the dry season (1.2–1.5 kPa) causes stomatal closure even in the absence of actual hydraulic stress. This sort of response is implicit in Jarvis-type stomatal conductance models, and the implied mechanism is a direct response of the guard cells to VPD. A second possible explanation, invoked by Tardieu (1993), involves the chemical signalling of soil water status, whereby abscisic acid is produced in root tissue in dry conditions and transported to the stomata, where it invokes stomatal closure (Zhang & Davies 1989). The sap flow velocities measured in this study were sufficient to allow the transport of abscisic acid at a rate of 8–15 m d⁻¹, around the height of the smallest trees. This is not sufficient to allow abscisic acid to be the cause of afternoon stomatal closure or any sort of subdiurnal pattern. It is possible that the afternoon stomatal closure may be explained by an interaction between chemical and hydraulic signals, as described by Tardieu (1993). However, since we did not measure abscisic acid concentrations, and because the dis-

crepancy is only a minor one, the integration of additional hypotheses into the model is not a research priority at this stage.

We have shown here that it is possible to model leaf water potential dynamics, stomatal conductance and sap flow, given a knowledge of the soil water potential and soil-leaf hydraulic resistance. However, modelling the dynamics of the soil-to-leaf hydraulic resistance is a further challenge (Sperry *et al*. 1998; Williams *et al*. 2001a; Tuzet, Perrier & Leuning 2003; Misson *et al*. 2004). To reduce uncertainty in the modelling of leaf water potential, we recommend that efforts should be concentrated on the estimation of soil and plant hydraulic resistance dynamics.

Are changes in soil-to-leaf water supply dominated by changes in soil water potential or by soil hydraulic resistance?

We tested the impact of changing the model input variables from their wet to their dry season values to investigate which factor had the greatest impact on gas exchange. Water supply to leaves is proportional to both the Ψ_s to Ψ_l gradient and to $1/R$ (Eqn 1). R appears to be more sensitive to changes in ecosystem water status and therefore was the dominant cause of reduced water use during the dry season. There is a small change in the Ψ_s to Ψ_l gradient (an average factor of 2.2). while a large change in $1/R$ between seasons has been recorded (an average factor of 7.6) (Table 3). Altering the model input meteorology and LAI from wet to dry season caused an increase in the SPA-simulated sap flow (Table 5). Subsequently decreasing Ψ_s to dry season values caused only a very small reduction of 0.07 mm d^{-1} in the control plot and a larger decrease of 0.26 mm d^{-1} in the TFE plot. However, setting R to its dry season values caused the simulated sap flow to decrease by 0.23 and 1.07 mm d^{-1} in the control and TFE plots, respectively. Some authors (Donovan *et al*. 2001) have criticized the use of pre-dawn leaf water potential as a proxy for soil water potential, using plants from desert ecosystems which are prone to night-time transpiration. In this instance, we believe that sap flow reaches zero during the night and that night-time transpiration is unlikely. In addition, if errors were introduced by the disequilibrium between soil and leaf water potential, correction of this would have the effect of reducing the estimated soil water potential. In this case, this would decrease the impact of soil water potential on model predictions even further and would reinforce the conclusions already drawn.

In addition, this analysis indicates that very little restriction on sap flow occurred in the control plot even in the height of the dry season. The maximum unstressed sap flow in the control plot was 4.2 mm d^{-1}, compared with 3.9 mm d^{-1} when resistance and soil water potential were changed to their dry season values. This finding mirrors that of Carswell *et al*. (2002), who found no seasonality in the eddy covariance gas exchange measurements performed at a flux tower 1 km from the TFE experiment at Caxiuanõ.

If there is a major change in soil-to-leaf hydraulic resistance, is the change in resistance located above or below ground?

We have shown that ecosystem sap flow is sensitive to soil-to-leaf hydraulic resistance and that soil-to-leaf hydraulic resistance is highly variable both between trees and through time. If simulation of the supply of water to leaves is a realistic and accurate means of simulating tree and forest sap flow as demonstrated here, then the next goal of the development of hydraulic limitation simulation must be to develop a process-based model for the a priori prediction of soil-to-leaf hydraulic resistance from other ecosystem level data. To achieve this goal, we must first deduce which part of the SPA continuum provides the greatest resistance to water movements under hydraulically stressed conditions.

We found that during the wet season, the stem water potential measurements were very close to the soil water potential measurements, indicating that most of the soil-to-leaf hydraulic resistance was located above ground. However, the main change in resistance between seasons was located below ground. The optimization of the parameter *b* indicated that an average of only 13% of the resistance was located below ground during the wet season, increasing to 45% during the dry season. Between seasons, the total soil-leaf resistance increase in all trees, except in trees C2 and T2. The total above-ground resistance did not change by more than 0.5 s MPa m^2 mmol^{-1} between seasons for all trees, except for trees T3 and T4. These results suggest that under control or ambient conditions, changes in R_{bg} are the dominating factor in the dry season response of the trees. Under some more extreme dry conditions in the TFE plot, some increase in R_{ag} was triggered by the low system water potential. Branch resistivity values indicate no change in above-ground resistance between seasons.

We have therefore found that changes in below-ground resistance are the likely cause of stomatal limitation in the dry season. It remains to be determined whether this is due to increases in root xylem or soil-to-leaf hydraulic resistance.

CONCLUSIONS

We tested the hypothesis that stomata function to maintain isohydric conditions in rain forest trees under hydraulically stressed situations. We tested this hypothesis against diurnal time series in leaf water potential, stomatal conductance, sap flow and stem water potential from a tropical rain forest. The hypothesis, as embedded in the SPA model and including no optimized parameters, is in broad agreement with the data. Further model analyses indicate that variations in soil-to-leaf resistance are the major factor that limits water use during the dry season and that very little hydraulic limitation of sap flow occurred in the control plot during the dry season. Stem psychrometer measurements indicate that the major change in resistance between seasons is located below ground, and we suggest that advances in understanding the response of tropical forests to gas

exchange will result from intensification of research on the dynamics of soil-to-leaf hydraulic resistance.

We expect that increasing confidence in process-based representations of drought stress will eventually allow identification of the critical factors that controls forest vulnerability to drought stress. This will allow integration of our increasing understanding of forest hydrology and gas exchange processes with our concern about the effect of drier climates on biosphere–atmosphere interactions, both within Amazonia and in other drought-threatened ecosystems.

ACKNOWLEDGMENTS

REFERENCES

Avissar R. & Nobre C.A. (2002) Preface to special issue on the Large-Scale Biosphere-Atmosphere Experiment in Amazonia (LBA). *Journal of Geophysical Research* **107,** 8034. doi:10.1029/2002JD002507.

Bonal D., Barigah T.S., Granier A. & Guehl J.M. (2000) Late-stage canopy tree species with extremely low delta C-13 and high stomatal sensitivity to seasonal soil drought in the tropical rain forest of French Guiana. *Plant, Cell and Environment* **23,** 445–459.

Carswell F.E., Costa A.L., Palheta M., *et al.* (2002) Seasonality in CO_2 and H_2O flux at an eastern Amazonian rain forest. *Journal of Geophysical Research* **107,** 8076.

Cermak J., Deml M. & Penka M. (1973) New method of sap flow-rate determination in trees. *Biologia Plantarum* **15,** 171–178.

Cermak J., Kucera J. & Nadezhdina N. (2004) Sap flow measurements with some thermodynamic methods, flow integration within trees and scaling up from sample trees to entire forest stands. *Trees – Structure and Function* **18,** 529–546.

Chaves M.M., Maroco J.P. & Pereira J.S. (2003) Understanding plant responses to drought – from genes to the whole plant. *Functional Plant Biology* **30,** 239–264.

Cochard H., Breda N. & Granier A. (1996) Whole tree hydraulic conductance and water loss regulation in Quercus during drought: evidence for stomatal control of embolism? *Annales Des Sciences Forestieres* **53,** 197–206.

Comstock J. & Mencuccini M. (1998) Control of stomatal conductance by leaf water potential in *Hymenoclea salsola* (T. & G.), a desert subshrub. *Plant, Cell and Environment* **21,** 1029–1038.

Cowling S.A., Betts R.A., Cox P.M., Ettwein V.J., Jones C.D., Maslin M.A. & Spall S.A. (2004) Contrasting simulated past and future responses of the Amazonian forest to atmospheric change. *Philosophical Transactions of the Royal Society of London Series B – Biology Science* **359,** 539–547.

Cox P.M., Betts R.A., Jones C.D., Spall S.A. & Totterdell I.J. (2000) Acceleration of global warming due to carbon-cycle feedbacks in a coupled climate model. *Nature* **408,** 184–187.

Cox P.M., Betts R.A., Collins M., Harris P.P., Huntingford C. & Jones C.D. (2004) Amazonian forest dieback under climate-carbon cycle projections for the 21st century. *Theoretical and Applied Climatology* **78,** 137–156.

Cramer W., Bondeau A., Schaphoff S., Lucht W., Smith B. & Sitch S. (2004) Tropical forests and the global carbon cycle: impacts of atmospheric carbon dioxide, climate change and rate of deforestation. *Philosophical Transactions of the Royal Society of London Series B – Biology Science* **359,** 331–343.

Cubasch U., Meehl G.A. & Boer G.J. *et al.* (2001) Projections of future climate change. In *Climate Change 2001: The Scientific Basis. Contribution of Working Group I to the Third Assessment Report of the Intergovernmental Panel on Climate Change* (eds J.T. Houghton, Y. Ding, M. Griggs), pp. 525–582. Cambridge University Press, Cambridge, UK.

Donovan L.A., Linton M.J. & Richards J.H. (2001) Predawn plant water potential does not necessarily equilibrate with soil water potential under well-watered conditions. *Oecologia* **129,** 328–335.

Farquhar G.D., & Caemmerer S.V. (1980) A biochemical model of photosynthetic CO_2 assimilation in leaves of C3 species. *Planta* **149,** 78–90.

Field C.B. & Holbrook N.M. (1989) Catastrophic xylem failure: tree life at the brink. *Trends in Ecology and Evolution* **4,** 124–126.

Goldstein G., Andrade J.L., Meinzer F.C., Holbrook N.M., Cavelier J., Jackson P. & Celis A. (1998) Stem water storage and diurnal patterns of water use in tropical forest canopy trees. *Plant, Cell and Environment* **21,** 397–406.

Goulden M.L., Miller S.D., da Rocha H.R., Menton M.C., de Freitas H.C., Figueira A.M.E.S. & de Sousa C.A.D. (2004) Diel and seasonal patterns of tropical forest CO_2 exchange. *Ecological Applications* **14,** S42–S54.

Hubbard R.M., Ryan M.G., Stiller V. & Sperry J.S. (2001) Stomatal conductance and photosynthesis vary linearly with plant hydraulic conductance in ponderosa pine. *Plant, Cell and Environment* **24,** 113–121.

Irvine J. & Grace J. (1997) Continuous measurements of water tensions in the xylem of trees based on the elastic properties of wood. *Planta* **202,** 455–461.

Jones H.G. (1992) *Plants and Microclimate*. Cambridge University Press, Cambridge, UK.

Jones H.G. (1998) Stomatal control of photosynthesis and transpiration. *Journal of Experimental Botany* **49,** 387–398.

Jones H.G. & Sutherland R.A. (1991) Stomatal control of xylem embolism. *Plant, Cell and Environment* **14,** 607–612.

Malhi Y., Nobre A.D., Grace J., Kruijt B., Pereira M.G.P., Culf A. & Scott S. (1998) Carbon dioxide transfer over a Central Amazonian rain forest. *Journal of Geophysical Research – Atmospheres* **103,** 31.593–31.612.

Malhi Y., Pegoraro E., Nobre A.D., Pereira M.G.P., Grace J., Culf A.D. & Clement R. (2002) Energy and water dynamics of a central Amazonian rain forest. *Journal of Geophysical Research – Atmospheres* **107,** doi: 10.1029/2001JD000623.

Mencuccini M. (2002) Hydraulic constraints in the functional scaling of trees. *Tree Physiology* **22,** 553–565.

Misson L., Panek J.A. & Goldstein A.H. (2004) A comparison of three approaches to modeling leaf gas exchange in annually drought-stressed ponderosa pine forests. *Tree Physiology* **24,** 529–541.

Oren R., Phillips N., Ewers B.E., Pataki D.E. & Megonigal J.P.

(1999) Sap-flux-scaled transpiration responses to light, vapor pressure deficit, and leaf area reduction in a flooded *Taxodium distichum* forest. *Tree Physiology* **19**, 337–347.

da Rocha H.R., Goulden M.L., Miller S.D., Menton M.C., Pinto L.D.V.O., de Freitas H.C. & Figueira A.M.E.S. (2004) Seasonality of water and heat fluxes over a tropical forest in eastern Amazonia. *Ecological Applications* **14**, S22–S32.

Ruivo M.L.P. & Cunha E.S. (2003) Mineral and organic components in archaeological black earth and yellow latosol in Caxiuanã, Amazon, Brazil. In *Ecosystems and Sustainable Development* (eds E. Tiezzi, C.A. Brebbia & J.L. Uso), pp. 1113–1121. WIT Press, Southampton, UK.

Saleska S.R., Miller S.D., Matross D.M. *et al.* (2003) Carbon in amazon forests: unexpected seasonal fluxes and disturbance-induced losses. *Science* **302**, 1554–1557.

Saliendra N.Z., Sperry J.S. & Comstock J.P. (1995) Influence of leaf water status on stomatal response to humidity, hydraulic conductance, and soil drought in *Betula occidentalis*. *Planta* **196**, 357–366.

Salleo S., Nardini A., Pitt F. & Lo Gullo M.A. (2000) Xylem cavitation and hydraulic control of stomatal conductance in Laurel (*Laurus nobilis* L.). *Plant, Cell and Environment* **23**, 71–79.

Sperry J.S. & Tyree M.T. (1988) Mechanism of water stress-induced xylem embolism. *Plant Physiology* **88**, 581–587.

Sperry J.S., Adler F.R., Campbell G.S. & Comstock J.P. (1998) Limitation of plant water use by rhizosphere and xylem conductance: results from a model. *Plant, Cell and Environment* **21**, 347–359.

Sperry J.S., Hacke U.G., Oren R. & Comstock J.P. (2002) Water deficits and hydraulic limits to leaf water supply. *Plant, Cell and Environment* **25**, 251–263.

Tardieu F. (1993) Will increases in our understanding of soil-root relations and root signaling substantially alter water flux models? *Philosophical Transactions of the Royal Society of London Series B – Biological Sciences* **341**, 57–66.

Tuzet A., Perrier A. & Leuning R. (2003) A coupled model of stomatal conductance, photosynthesis and transpiration. *Plant, Cell and Environment* **26**, 1097–1116.

Tyree M.T. & Sperry J.S. (1988) Do woody-plants operate near the point of catastrophic xylem dysfunction caused by dynamic water stress – answers from a model. *Plant Physiology* **88**, 574–580.

Williams M., Rastetter E.B., Fernandes D.N., Goulden M.L., Wofsy S.C., Shaver G.R., Melillo J.M., Munger J.W., Fan S.M. & Nadelhoffer K.J. (1996) Modelling the soil–plant–atmosphere continuum in a *Quercus-Acer* stand at Harvard Forest: the regulation of stomatal conductance by light, nitrogen and soil/plant hydraulic properties. *Plant, Cell and Environment* **19**, 911–927.

Williams M., Malhi Y., Nobre A.D., Rastetter E.B., Grace J. & Pereira M.G.P. (1998) Seasonal variation in net carbon exchange and evapotranspiration in a Brazilian rain forest: a modelling analysis. *Plant, Cell and Environment* **21**, 953–968.

Williams M., Eugster W., Rastetter E.B., McFadden J.P. & Chapin F.S. (2000) The controls on net ecosystem productivity along an Arctic transect: a model comparison with flux measurements. *Global Change Biology* **6**, 116–126.

Williams M., Law B.E., Anthoni P.M. & Unsworth M.H. (2001a) Use of a simulation model and ecosystem flux data to examine carbon–water interactions in ponderosa pine. *Tree Physiology* **21**, 287–298.

Williams M., Bond B.J. & Ryan M.G. (2001b) Evaluating different soil and plant hydraulic constraints on tree function using a model and sap flow data from ponderosa pine. *Plant, Cell and Environment* **24**, 679–690.

Zhang J. & Davies W.J. (1989) Abscisic acid produced in dehydrating roots may enable the plant to measure the water status of the soil. *Plant, Cell and Environment* **12**, 73–81.

Zwieniecki M.A. & Holbrook N.M. (2000) Bordered pit structure and vessel wall surface properties: implications for embolism repair. *Plant Physiology* **123**, 1015–1020.

APPENDIX

We used an estimate of capacitance (*C*) derived using the data of Goldstein *et al.* (1998) for a seasonal tropical forest in Panama, the only published estimate of *C* for tropical forest trees. Goldstein *et al.* (1998) found a relationship between tree basal area and tree capacitance by measuring the lag between sap flow in terminal branches and at the base of the trunk. We converted these estimates of *C* to the units required for SPA, using Eqn 5:

$$C = \frac{1}{n} \sum \frac{c_i}{r \Psi_{\text{min,i}}} \tag{5}$$

where *C* is the new value of capacitance [mmol MPa^{-1} m^{-2} (leaf area)], c_i is the value of capacitance [mmol m^{-2} (basal area)] calculated by Goldstein *et al.* (1998) for the *i*th tree, Ψ_{min} is the minimum value of Ψ_1 reported by Goldstein *et al.* for the *i*th tree (MPa), *n* is the number of trees sampled and *R* is the ratio between basal area and leaf area calculated for our site (5.5 m^2 m^{-2}). The sensitivity of soil–plant–atmosphere (SPA) to *C* is low, except at the extremes of the ranges (Williams *et al.* 1998), so this method of calculation, using data from elsewhere in the tropics, is a tolerable level of uncertainty, given that there are no other data sets available for tropical species. Using this method, we find a mean value of *C* of 2300 mmol m^{-2} MPa^{-1}.

The simulated sap flow (S_j) in mm h^{-1} was calculated as shown in Eqn 6.

$$S_j = \sum_{i=l_j}^{h_j} \frac{s_i L_{j,i}}{l_i} \tag{6}$$

where *j* is a given tree and *i* is one of the 10 modelled canopy layers. s_i is the SPA-simulated sap flow (mm h^{-1} m^{-2} – ground area) of layer *i*. l_i is the modelled leaf area (m^{-2}) in layer *i* per m^{-2} of ground area. $L_{i,j}$ is the leaf area estimated for layer *i* of tree *j* (m^{-2}).